EARTH SCIENCES
UNIVERSITY OF MINNESOTA

The SPARC Data Center and Stratospheric Precursors for Tropospheric Phenomena

Stefan Liess[1] and Marvin A. Geller[2]

[1]Department of Earth Sciences - University of Minnesota, Minneapolis, MN 55455 - liess@umn.edu
[2]Institute for Terrestrial and Planetary Atmospheres, Stony Brook University, Stony Brook, NY 11794-5000

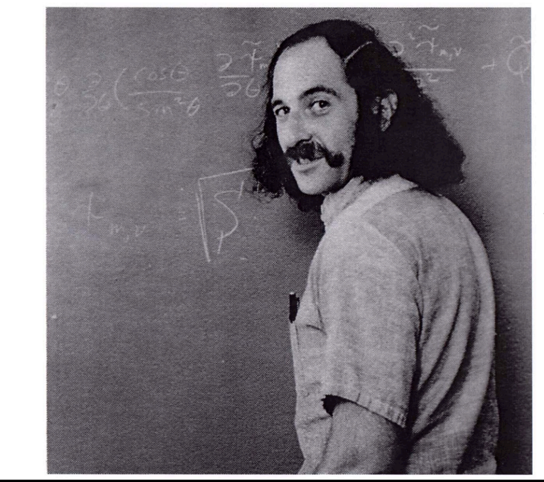

INSTITUTE FOR TERRESTRIAL AND PLANETARY ATMOSPHERES
STONY BROOK
STATE UNIVERSITY OF NEW YORK

THE SPARC DATA CENTER:

The Stratosphere-troposphere Processes And their Role in Climate (SPARC) Data Center at http://www.sparc-climate.org/data-centre (QR-code on right) is working with various SPARC projects to acquire newly available data and to maintain archives of existing data that have been used in past projects. Funding is made available by NASA and NSF.

Selected SPARC Data Holdings:

- **High-Resolution 1 sec (6 sec) Radiosonde Data** from 93 US operated stations for **2005-2011 (1998-2011)** (Love and Geller, 2013)
- **Ozone trends** 1979-2005 (Randel and Wu, 1999; 2007)
- **Assessment of Stratospheric Aerosol Properties (ASAP)** (SPARC, 2006)
- **Rocketsonde Data** for 1957-1992 (Baldwin and Gray, 2004)
- **Quantum Yields for Production of O(1D) In The Ultraviolet Photolysis Of Ozone:** Table of recommended values and a fitting expression depending on photolysis wavelength and temperature (Matsumi et al., 2002)
- **Small Organic Peroxy Radicals:** Reaction rate coefficients and products recommended for use in atmospheric modeling of CH3O2, C2H5O2, CH3C(O)O2, and CH3C(O)CH2O2 (Tyndall et al., 2001)
- **Climate Forcing Parameters** that influence stratospheric change (Karoly, 2000)
- **Tropical Tropopause, Tropospheric and Stratospheric Climatologies** from Radiosondes (Seidel et al., 2001)
- **Trace Gas Climatologies** from HALOE, CLAES, and MLS (Randel et al., 1998)
- SPARC **Water Vapour Assessment** (WAVAS-1) (SPARC, 2000)
- SPARC **Reference Climatology Intercomparison Project** (Swinbank and Ortland 2003; and others)
- **Tropopause Height Climatologies** Randel et al. (2000)
- **GCM–Reality Intercomparison Project for SPARC** (GRIPS) (Pawson et al. 2000)

Responsible Scientists: Petra M. Udelhofen † (1999-2002), Xuelong Zhou (2002-2004), Stefan Liess (2004-2009), Peter T. Love (2009-present)

Hardware at SBU(1999-2007)	Hardware at SBU(2007-pres.)	Merged Hardware (2014-pres.)
Dell Power Edge 4300 Workstation • 500 MHz dual processor Pentium III • RAID5 array for storage of up to155 Gb • Built-in CD writer, DAT tape drive • Backups on DDS-3 4mm tape cartridges 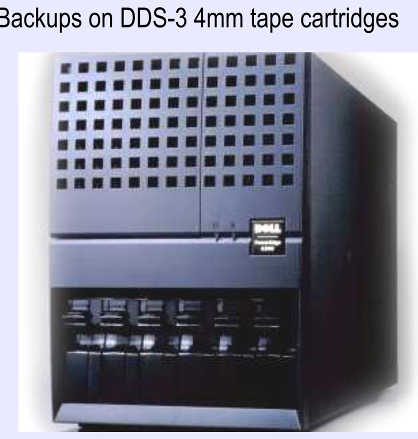	**Dell PowerEdge 2900 III Server** • 2 x 2.5 GHz AMD Opteron quadcore processors (x 20 increase) • RAID5 array for storage of up to 4 Tb disk space (x 26 increase) • ftp://atmos.sparc.sunysb.edu/pub/sparc **PowerVault V110T, LTO-3 Tape Backup** 1 cartridge slot for capacity up to 800 GB (compressed) (x 33 increase) 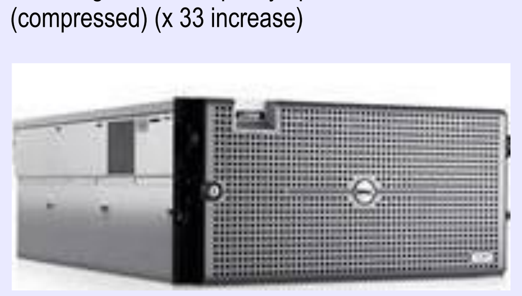	**SPARC DC merged with BADC and NEODC to CEDA** • The previous server still serves as mirror / backup. • CEDA has over 1Pb of data stored in more than 100 million files. • CEDA includes British Atmospheric Data Centre, NERC Earth Observation Data Centre, and SPARC Data Centre. • http://www.sparc-climate.org/data-centre • ftp://sparc-ftp1.ceda.ac.uk Centre for Environmental Data Archival SCIENCE AND TECHNOLOGY FACILITIES COUNCIL NATURAL ENVIRONMENT RESEARCH COUNCIL

REFERENCES

Baldwin, M. P. and T. J. Dunkerton (2001): Stratospheric harbingers of anomalous weather regimes. Science, 294, 581-584.
Collimore, C. C., D. W. Martin, M. H. Hitchman, A. Huesmann and D. E. Waliser (2003): On the relationship between the QBO and Tropical deep convection. J. Climate, 16, 2552-2568.
Karoly, D.J. (2000): Stratospheric aspects of climate forcing. SPARC Newsletter, 14.
Liess, S. and M.A. Geller (2012): On the relationship between QBO and distribution of tropical deep convection. J. Geophys. Res., 2012. 117, D03108.
Liess, S. et al. (2014): Different modes of variability over the Tasman Sea: Implications for regional climate. J. Climate, 27: p. 8466-8486.
Liess, S., S. Agrawal, S. Chatterjee and V. Kumar (2016): A teleconnection between the West Siberian Plain and the ENSO region. J. Climate, submitted.
Love, P. T. and M. A. Geller (2013): Exploring and improving access to high vertical resolution radiosonde data. Eos Transactions, AGU, 94, 401.
Matsumi, Y. et al. (2002): Quantum yields for production of O(1D) in the ultraviolet photolysis of ozone: Recommendation based on evaluation of laboratory data, J. Geophys. Res., 107.
Pawson, S. et al. (2000): The GCM-Reality Intercomparison Project for SPARC (GRIPS): Scientific issues and initial results. Bull. Amer. Meteorol. Soc., 81, 781-796.
Randel, W. J. and F. Wu (1999): A stratospheric ozone trends data set for global modelling studies. Geophys. Res. Lett., 26, 3089-3092.
Randel, W.J., F. Wu and D. Gaffen (2000): Interannual variability of the tropical tropopause derived from radiosonde data and NCEP reanalyses. J. Geophys. Res., 105, 15509-15523.
Randel, W. J. and F. Wu (2007): A stratospheric ozone profile data set for 1979–2005: Variability, trends, and comparisons with column ozone data, J. Geophys. Res., 112, D06313.
Rossow, W. B., G. Tselioudis, A. Polak and C. Jakob (2005): Tropical climate described as a distribution of weather states indicated by distinct mesoscale cloud property mixtures. Geophys. Res. Lett., 32, L21812.
Seidel, D.J., R.J. Ross, J.K. Angell and G.C. Reid (2001): Climatological characteristics of the tropical tropopause as revealed by radiosondes. J. Geophys. Res., 106, 7857-7878.
SPARC Report No. 2 (2000): Upper Tropospheric and Stratospheric Water Vapour. D. Kley, J.M. Russell III, and C. Philips (eds.). WCRP-113, WMO/TD - No. 1043.
SPARC Report No. 4 (2006): Assessment of Stratospheric Aerosol Properties (ASAP). L. Thomason and Th. Peter (Eds.), WCRP-124, WMO/TD - No. 1295.
Swinbank, R. and D.A. Ortland (2003): Compilation of wind data for the UARS Reference Atmosphere Project, J. Geophys. Res., 108, D19, 4615.
Thompson, D. W. J., M. P. Baldwin and S. Solomon (2005): Stratosphere–troposphere coupling in the Southern Hemisphere. J. Atmos. Sci., 62, 708-715.
Tyndall, G.S., R.A. Cox, C. Granier, R. Lesclaux, G.K. Moortgat, M.J. Pilling, A.R. Ravishankara and T.J. Wallington (2001): Atmospheric chemistry of small organic peroxy radicals, J. Geophys. Res. 106, 12,157-12,182.
Zhou, X., M. A. Geller and M. Zhang (2001): Tropical cold point tropopause characteristics derived from ECMWF reanalyses and soundings. J. Climate, 14, 1823-1838.

STRATOSPHERIC PRECURSORS:

Three independent phenomena with stratosphere/troposphere interaction are introduced: **I:** The quasi-biennial oscillation (QBO) is associated to wind fields that must extend down below the tropopause given that a QBO variation is seen in the tropical tropopause (e.g. Zhou et al., 2001). Liess and Geller (2012) used 21.5 years (1983–2004) of daily ISCCP Weather States (Rossow et al., 2005) **(Fig. 1)** to show how the QBO **(Fig. 2)** modulates tropical deep convection **(Fig. 3).** The relative differences in convective cloud cover between the QBO easterly and QBO westerly phases can be as large as 51%±7% over isolated regions in the tropical west Pacific and 103%±35% over the east Pacific. The Hadley cell is strengthened (weakened) over the west (east) Pacific during the QBO easterly phase. **II:** A teleconnection pattern near the Tasman Sea (Liess et al. 2014) **(Fig. 4)** is related to the Southern Annular Mode (SAM, Thompson et al., 2005) and occurs in the lower stratosphere during southern fall and winter. It is present throughout the year in the troposphere **(Fig. 5)** where it affects drought conditions over Australia **(Fig. 6).** **III:** Liess et al. (2016) show a teleconnection pattern between the West Siberian Plain and the ENSO region (represented by two regions around Darwin, Australia and Tahiti) **(Fig. 7)** that is related to the Northern Annular Mode (NAM, Baldwin and Dunkerton 2001). During DJF, a circumglobal wavetrain **(Fig. 8)** is reflected in the polar region near the West Siberian Plain, where the stratospheric circulation modulates its connection to the ENSO region **(Fig. 9).**

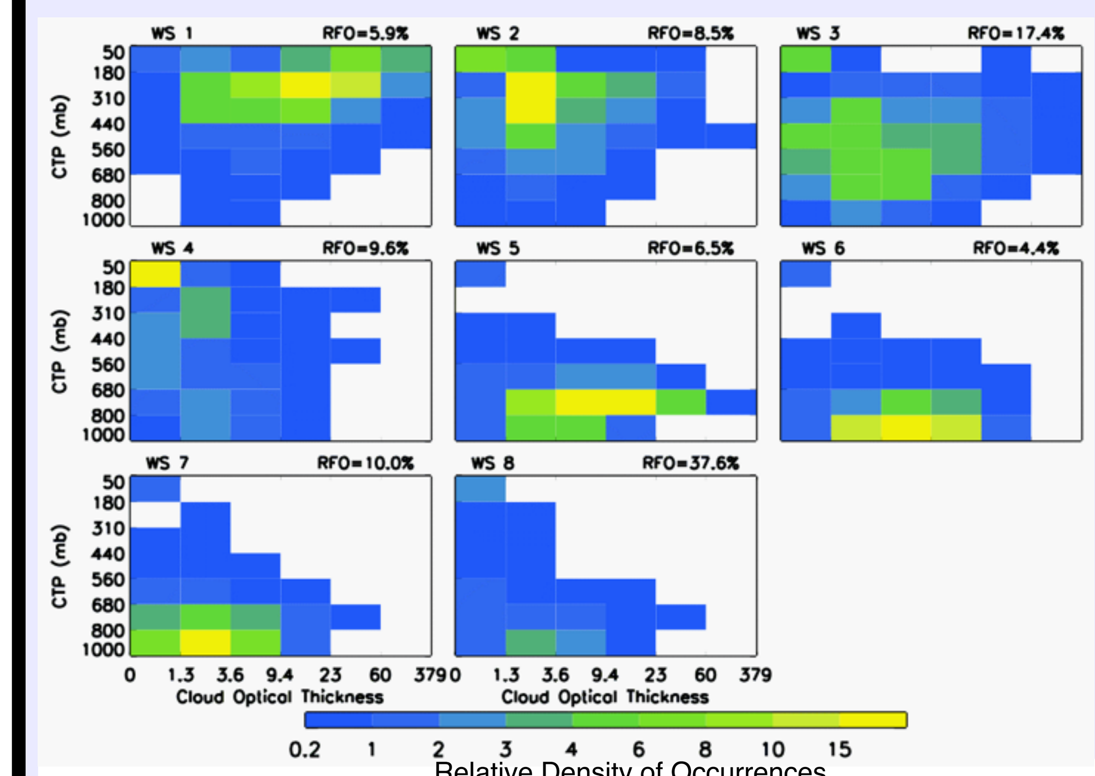

Figure 1. Frequency histograms (Weather States) for tropical convection based on optimum cluster centroids for ISCCP D1 data between 35ºN and 35ºS (from http://isccp.giss.nasa.gov/etcluster.html). WS1 and WS2: deep convection, WS4: cirrus.

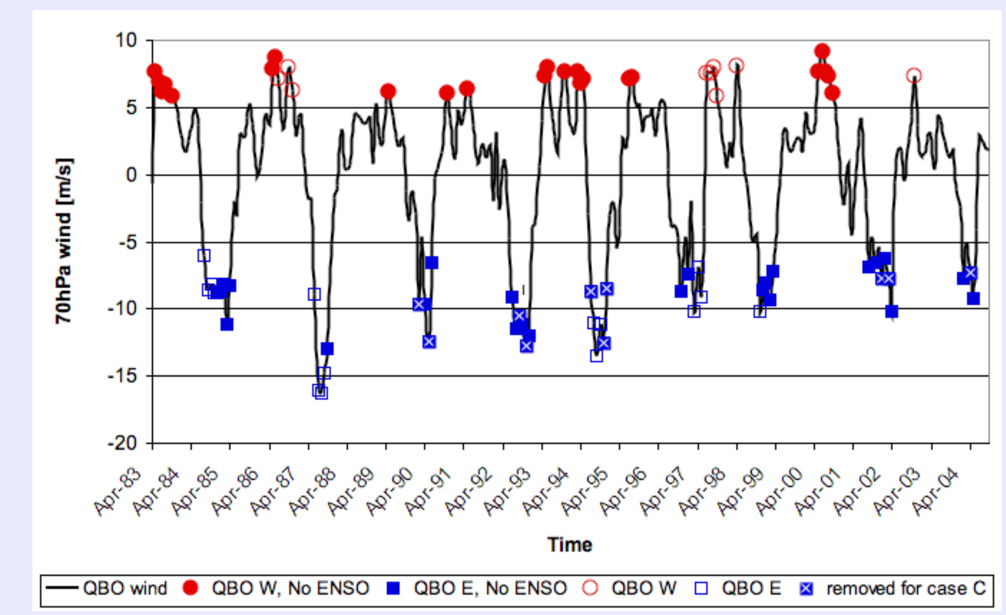

Figure 2. 70-hPa zonal wind from http://www.geo.fu-berlin.de/met/ag/strat/produkte/qbo/qbo.dat (Naujokat, 1986). Marks show pos. and neg. QBO phases. Open (crossed) marks are removed from consideration as ENSO events (SST adjustment for equal avg. NINO3.4 SST in pos. and neg. phases).

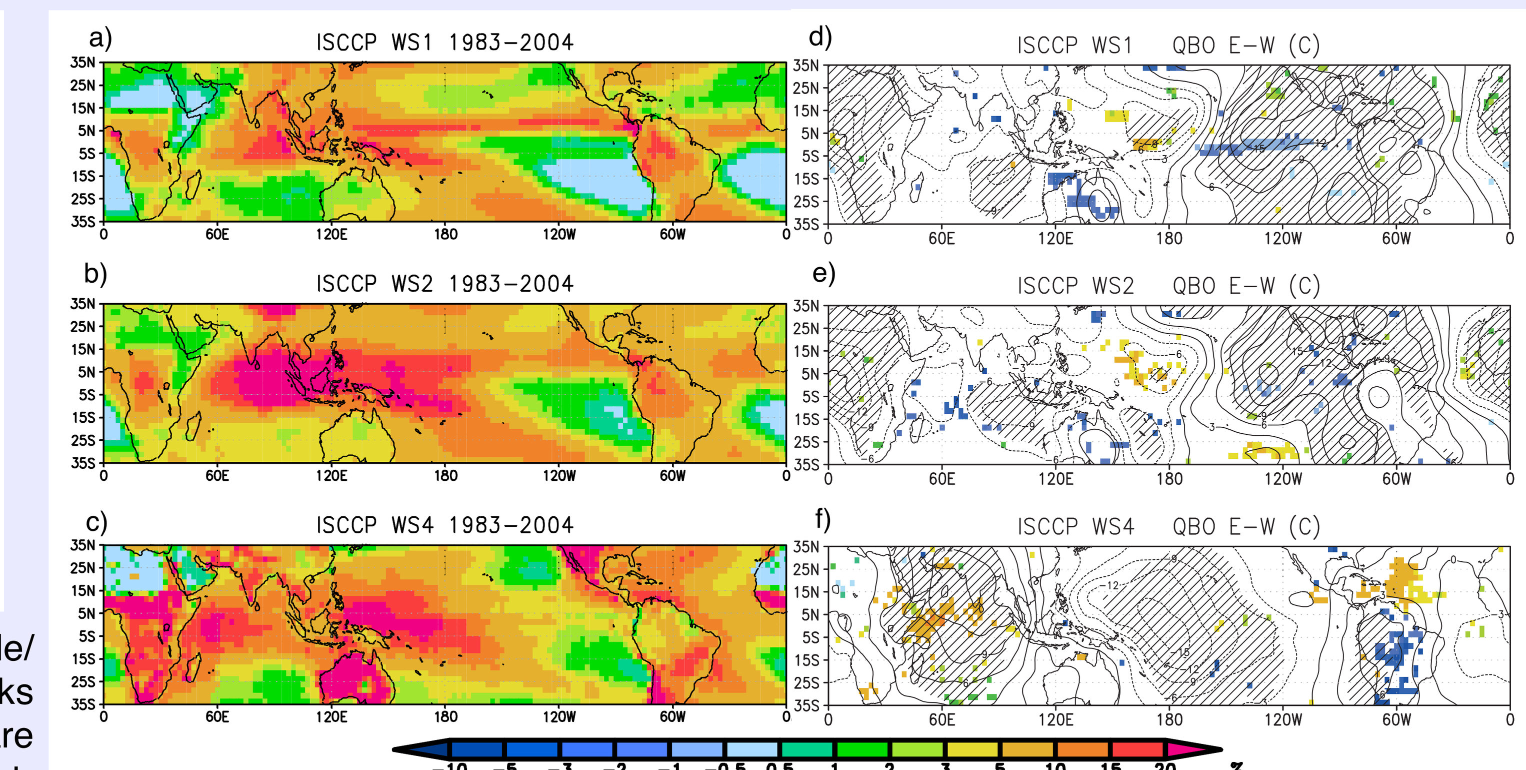

Figure 3. Absolute values of frequency of occurrence of (a) mature deep convection WS1, (b) growing deep convection WS2, and (c) cirrus clouds WS4, and (d–f) their respective differences between QBO easterly (neg.) and westerly (pos.) phase. Only statistically significant values are shown in Figures 3d–3f. Respective NCEP velocity potential differences (contour) at (d) 150 hPa, (e) 200 hPa, and (f) 100 hPa represent the upper limit of WS1, WS2, and WS4 occurrence (see Fig. 1). The contour interval is $3{*}10^5$ m^2 s^{-1} with neg. values being dashed. Statistically significant values are hatched.

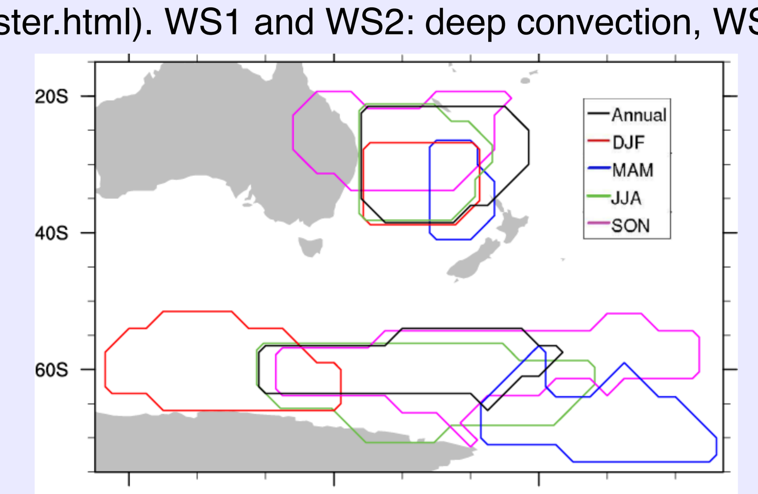

Figure 4. Northern and southern centers of a teleconnection found with a shared reciprocal nearest neighbors (Kawale et al. 2013) approach in all four seasons. The teleconnection is influenced by SAM, ENSO, and the Indian Ocean Dipole (IOD).

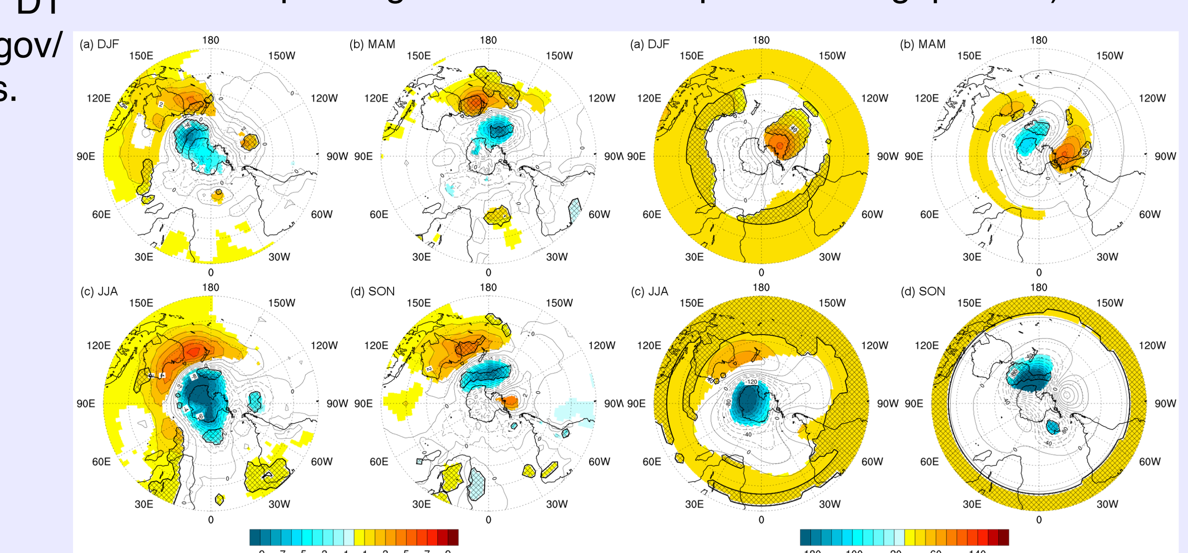

Figure 5. (Left) HadSLP2 differences in hPa and (right) 50-hPa geopotential height differences in m between pos. and neg. teleconnection phases during four seasons. Shading indicates significance using a t-test at a 95% confidence level. Hatching represents areas that are significant for this teleconnection but not for SAM, ENSO, or IOD.

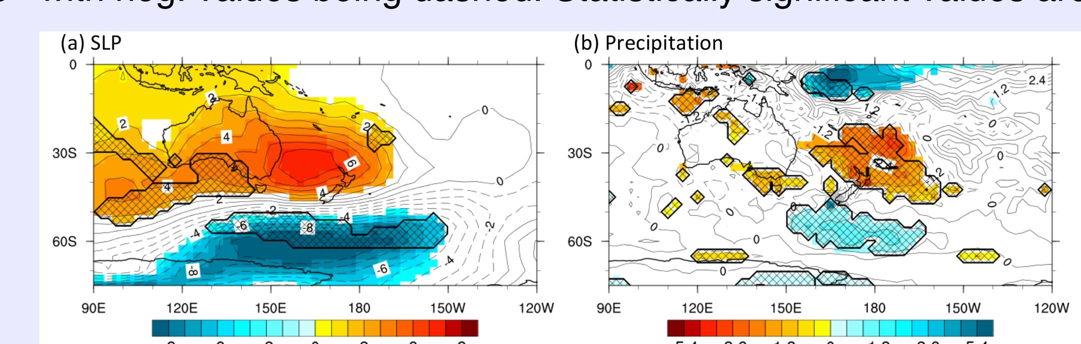

Figure 6. As Fig. 5, but for annual (a) HadSLP2 (hPa) and (b) GPCP precipitation (mm day^{-1}) differences for thresholds of twice the standard deviation.

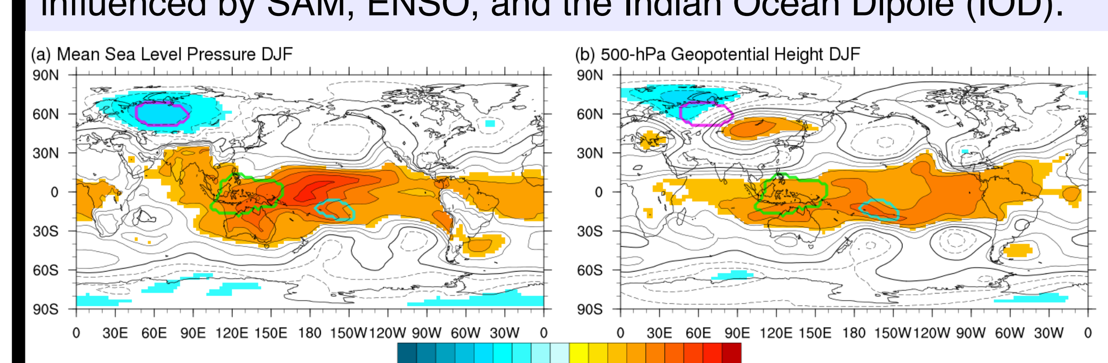

Figure 7. MERRA SLP tripole between west Pacific warm pool (R1=green), central Pacific (R2=cyan), and northern Russia (R3=magenta) during DJF. Contours indicate the correlation values of (a) SLP and (b) 500-hPa geopotential height with the R1+R2 time series. The zero line is thickened and negative contours are dashed. Statistically significant correlations at the 95% confidence interval are shaded.

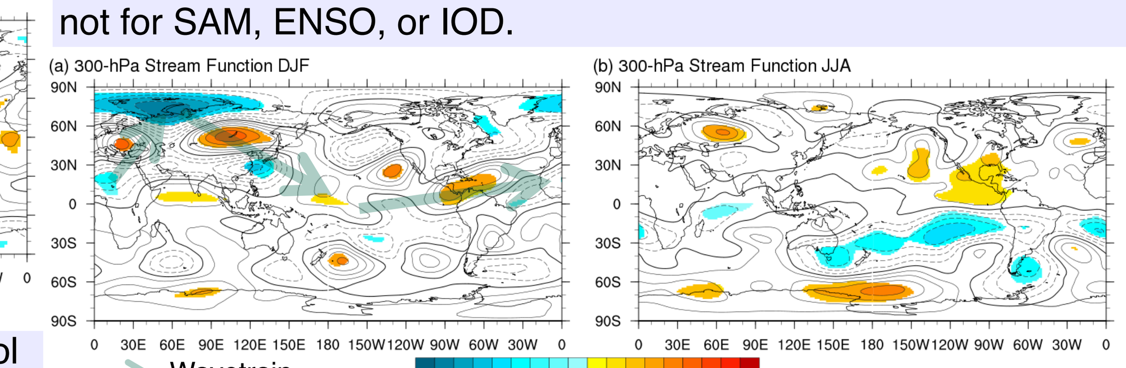

Figure 8. MERRA 300-hPa stream function in m^2 s^{-1} composite analysis for positive minus negative index phases of time series over R1+R2 during DJF and JJA. The zero line is thickened and negative contours are dashed. Shading indicates significance using a t-test at a 95% confidence level.

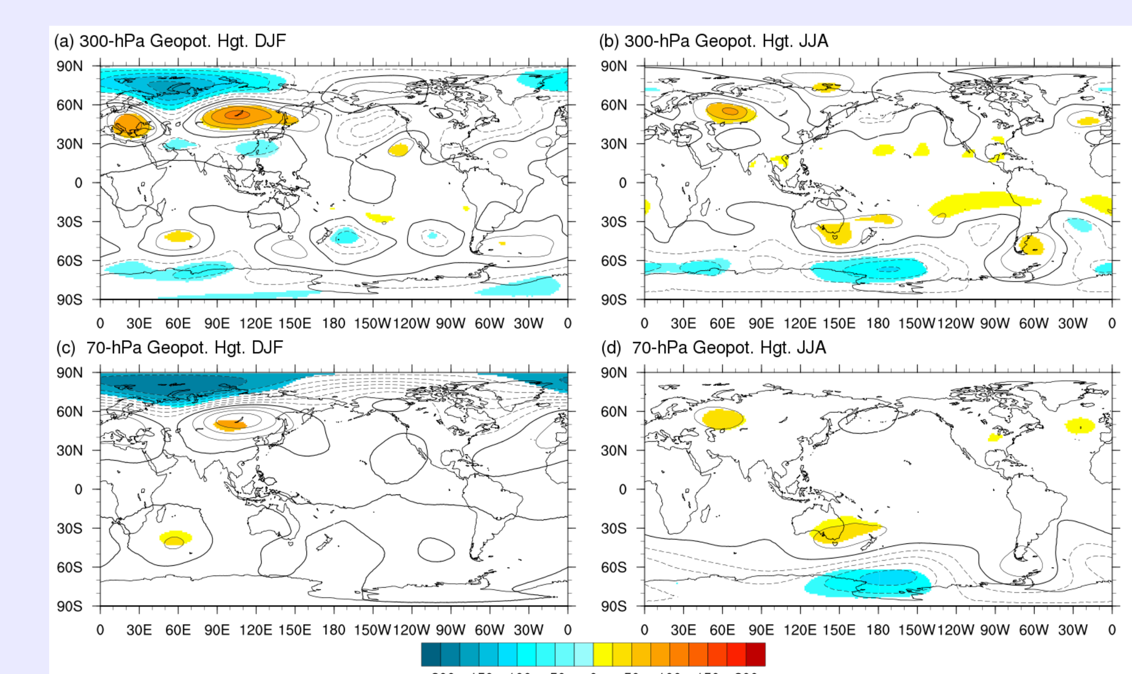

Figure 9. As Fig. 8, but for geopotential height in m.